JOURNAL OF CATALYSIS 154, 194–200 (1995)

Study of the Real Structure of Silver Supported Catalysts of Different Dispersity

S. V. Tsybulya,[1] G. N. Kryukova, S. N. Goncharova, A. N. Shmakov, and B. S. Bal'zhinimaev

Boreskov Institute of Catalysis, Siberian Branch of Russian Academy of Sciences, pr. Lavrentieva 5, Novosibirsk 630090, Russia

Received May 16, 1994; revised December 9, 1994

The real structure of silver supported catalysts for ethylene epoxidation (Ag/α-Al_2O_3) was investigated using precision X-ray diffraction on synchrotron radiation, *in situ* high-temperature X-ray diffraction, and transmission electron microscopy. Stacking faults and intergrain boundaries were found to be main types of defects in the structure of silver microcrystals. *In situ* study revealed that under reaction conditions the intergrain boundaries remain unchanged, whereas stacking faults are annealed. We found a correlation between the reaction rate of ethylene epoxidation and parameters responsible for the relationship among the regular and defect regions in the bulk structure of silver particles. © 1995 Academic Press, Inc.

INTRODUCTION

Ag/α-Al_2O_3 catalysts have great industrial importance in the process of ethylene epoxidation. One of the well-known properties of silver supported catalysts is the observed effect of silver particle size on the reaction rate (1–7). However, the nature of this dependence remains unclear. Thus, the authors (8) have reported on the particle size effect for silver catalysts with a narrow size distribution of Ag particles. The rate of the epoxidation reaction does not change when the mean size of the Ag particles lies in the range from 500 to 1000 Å. But at silver particle sizes of less than 500 Å a more than a 20-fold decrease in epoxidation rate is observed, though the phase composition of the supported particles is identified as metallic silver according to data from X-ray diffraction.

The authors (8–10) have reported on the particle size dependence of the adsorption properties and electronic state of supported silver. According to the data in these papers, the structural change in the surface layers of the Ag microcrystals in relation to their size may be one of the reasons for the observed size effect. Most likely this effect is caused by the change in the ratio of the regular and defect surface regions of the Ag particles. In turn, we suggest that the bulk structure of the metallic particles forming during catalyst preparation or under the reaction conditions may strongly affect the arrangement of the surface structure of the catalysts.

The major objective of the work described here is to study the real structure of silver particles within a narrow size distribution. For this purpose we used precision X-ray diffraction of synchrotron radiation (XRDSR), *in situ* high-temperature X-ray diffraction (XRD), and transmission electron microscopy (TEM).

METHODS

Catalyst Preparation and Testing

Specimens were prepared using the incipient wetness procedure (11). Silver was deposited via the impregnation of α-alumina support (according to the BET method, specific surface area is equal to 7 m^2g^{-1}) with the silver amine complex in ethanolamine having molar ratio Ag: $NH_2C_2H_4OH$ = 1 : 4. To obtain catalysts within a narrow particle size distribution we used two nontraditional procedures: (i) modification of the initial α-alumina support by treatment of CsOH solution followed by Cs removal; and (ii) adsorption–contact drying at room temperature. The first procedure allows the creation of surface centers for silver nucleation on the support. During adsorption–contact drying we mixed the wet sample with calcined SiO_2 granules. Due to intensive agitation (12), the moisture passed from catalyst to silica faster than when heated without agitation. The use of both procedures allowed the production of very homogeneous particle sizes (the deviation from average size did not exceed 30–40%). Methods of catalyst preparation and characterization are described in more detail elsewhere (8).

Reduction of the catalysts was performed at 90°C under vacuum. Then the samples were washed with the bidistilled water and dried in air at 240°C for 2 h (the temperature was raised to 240°C over 40 min). To prepare the catalysts with various silver contents and dispersity, we varied the concentration of the impregnating solution or repeated the impregnation procedure several times.

The catalytic activity was measured with a flow-circula-

[1] To whom correspondence should be addressed.

0021-9517/95 $12.00

tion technique (13) at 230°C and atmospheric pressure. At first, the catalyst placed in a quartz reactor was treated with $O_2 + N_2$ (7% O_2) flow for 2 h at 230°C. The reaction rate was measured at the same temperature after the steady state had been achieved (usually 3–6 h). The initial mixture composition was the following: 2% C_2H_4, 7% O_2, and the balance was N_2. The catalyst weight (0.5–2 g) and flow rate of the reaction mixture feed (2–20 liter h^{-1}) were chosen so that the ethylene conversion under the steady state did not exceed 10–15%.

Data on the Ag/α-Al_2O_3 samples and their catalytic activity are given in Table 1. The specific surface area of silver was measured by means of oxygen chemisorption.

XRDSR Measurements and TEM Analysis

A precision diffraction experiment was performed with high resolution powder diffraction and an anomalous scattering station at the Siberian Synchrotron Radiation Center (14). A perfect flat Ge (111) crystal analyzer on the diffracted beam provides the high instrumental resolution of this station. This allows one to obtain diffraction patterns with full width at half maximum about 0.02°–0.025° in the 2θ angular range from 20° to 70°.

A high instrumental resolution gives some advantages in the investigation of the supported silver catalysts. For example, X-ray diffraction peaks of alumina and silver are better resolved, as evident from Figs. 1a and 1b, which illustrate the portions of X-ray spectra obtained, respectively, with a conventional URD-63 diffractometer (graphite monochromator, wavelength, 1.3922 Å) and a synchrotron radiation station (wavelength, 1.5403 Å). Thus, the main advantages of synchrotron radiation diffraction in the study of silver supported catalysts are as follows:

(i) A high instrumental resolution that results in the separation of alumina and silver reflections;

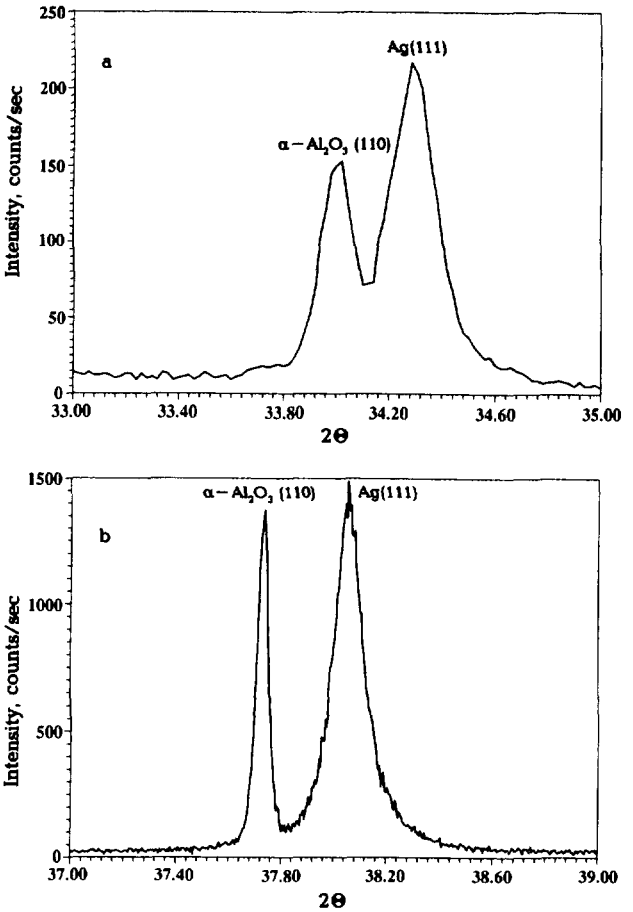

FIG. 1. Portions of X-ray diffraction spectra obtained with a conventional diffractometer (a) and station on synchrotron radiation (b).

(ii) A higher power of the radiation beam that registers diffraction peaks with low intensities;

(iii) The absence of systematic error in the determination of the positions of diffraction maxima. For conven-

TABLE 1

Physicochemical Characteristics of Ag/α-Al_2O_3 Catalysts and Their Catalytic Activity in the Reaction of Ethylene Epoxidation

Sample number	Support	Ag content (wt%)	Specific surface of Ag (m^2/g)	Reaction rate ($\times 10^{-17}$ molecule s^{-1} m^{-2})
1	α-Al_2O_3	1.8	0.46	0.65
2	—	2.4	0.75	0.20
3	—	2.7	0.50	0.60
4	—	3.5	0.80	0.03
5	—	3.7	0.53	1.90
6	—	6.5	0.93	2.30
7	—	8.1	0.58	3.80
8	—	8.1	0.32	5.40
9	—	13.8	0.62	4.90
10	No support	100	0.30	10.0

tional X-ray measurements such error is caused by the vertical divergence of the X-ray beam.

For the calculation of particle size, $D_{X\text{-ray}}$, we used Scherrer's equation, $D_{X\text{-ray}} = 0.9\ \lambda/\Delta(2\theta)\cos\theta$, where λ is a wavelength, $\Delta(2\theta)$ is a halfwidth of the diffraction peak, and θ is a position of the maximum of the diffraction peak. Microstrains in the structure of silver particles have been calculated based on the broadening of 111 and 222 diffraction reflections, using Cauchy's approximation (15).

In situ investigations were performed in an X-ray thermochamber at temperatures from 25 to 230°C. The volume of the thermochamber was equal to 10 cm^3. For the transmittance of X-ray radiation Be windows were used. The specimen was prepared in the form of a tablet with a diameter of 15 mm. The specimen was heated over the whole diameter of the cuvette. The temperature was raised from 25 to 230°C over 30 min. The specimen was heated in the thermochamber at 230°C for 2–4 h, which is close to the time for catalyst testing under the reaction conditions. The experiments were carried out in air and in under a reaction mixture with a composition of 2% C_2H_4 and 7% O_2 under He.

TEM investigations were performed with JEM-100C and JEM-4000EX electron microscopes. Initial catalysts, as well as samples obtained after *in situ* study, have been analyzed. Samples were prepared from the ethanol suspensions obtained by an ultrasonic treatment. Then a drop of suspension was placed on a copper grid covered with carbon film.

RESULTS

According to XRDSR, the phase composition of all samples in question corresponds to α-alumina and metallic silver. The crystal lattice parameters, which were obtained by the least-squares method from five diffraction reflections, of the Ag particles are similar to the JCPDS data file for metallic silver (a = 4.087(2) Å) (16).

The microstrain concentration was estimated using the diffraction peaks of two reflection orders, i.e., 111 and 222 reflections. The results of the calculations indicated that the concentration of microstrains for all initial samples is low ($\varepsilon \cong 10^{-4}$). This value corresponds to the equilibrium dislocation density ($\rho \cong 10^{-7}$ Å^{-2}). Thus, microstrains do not contribute to the broadening of the X-ray diffraction peaks that enables one to determine the particle sizes in the different crystallographic directions, $D_{X\text{-ray}}$, i.e., the sizes of the regions of silver particles possessing perfect (regular) crystal structure. Values of particle sizes, $D_{X\text{-ray}}$, calculated from the broadening of 111, 200, and 220 diffraction peaks are given in Table 2.

TABLE 2

Silver Particle Sizes Obtained from X-Ray Diffraction on Synchrotron Radiation and Transmission Electron Microscopy

Sample number	D_{111} (Å)	D_{200} (Å)	D_{220} (Å)	D_{TEM} (Å)	$D_{TEM}/D_{X\text{-ray}}$
1	180	—	160	225	1.2
2	200	—	170	185	0.9
3	300	270	320	310	1.0
4	280	250	230	250	0.9
5	250	150	180	400	1.55
6	280	235	200	400	1.4
7	470	290	390	780	1.65
8	720	430	520	1400	2.0
9	600	450	450	1000	1.7
10	860	670	740	>20000	—

This table also shows data on the mean Ag particle sizes obtained from the analysis of histograms (D_{TEM}).

Of most interest is the fact that values of $D_{X\text{-ray}}$ in all crystallographic directions in silver particles from certain samples are equal (see samples 3 and 4), whereas the same parameters differ from each other for other specimens, where maximum and minimum sizes are observed for 111 and 200 reflections, respectively. For samples 1 and 2, 200 diffraction peaks were so broadened that we have not been able to determine the halfwidths of these peaks. TEM revealed that there is no preferable orientation or shape anisotropy of silver particles in all the samples. As a rule, Ag microcrystals are in the form of hemispheres attached to the surface of the α-alumina support (see Fig. 2). Therefore, the distinctions in Ag particle sizes in different crystallographic directions result from the features of the real structure of Ag particles, i.e., the presence of stacking faults formed at the stage of the catalyst preparation. Indeed, one can see these defects (indicated by arrows) in the micrograph of the Ag particles shown in Fig. 3.

Metallic silver crystallizes in a face-centered cubic packing structure. For metals with this type of packing the presence of stacking faults situated in the plane perpendicular to the [111] direction slightly affects the broadening of the 111 diffraction peak (17). Therefore, the D_{111} value may be considered the most reliable indication of the size of the region of X-ray coherent scattering, $D_{X\text{-ray}}$. When $D_{X\text{-ray}}$ is noticeably smaller than D_{TEM}, the silver particle has an intergrained microstructure. In this case the Ag particle consists of several microcrystalline domains (see Fig. 4). The size of each domain is equal to that of the region of X-ray coherent scattering, $D_{X\text{-ray}}$, calculated from X-ray spectra. All domains are separated from each other by intergrain boundaries (indicated by

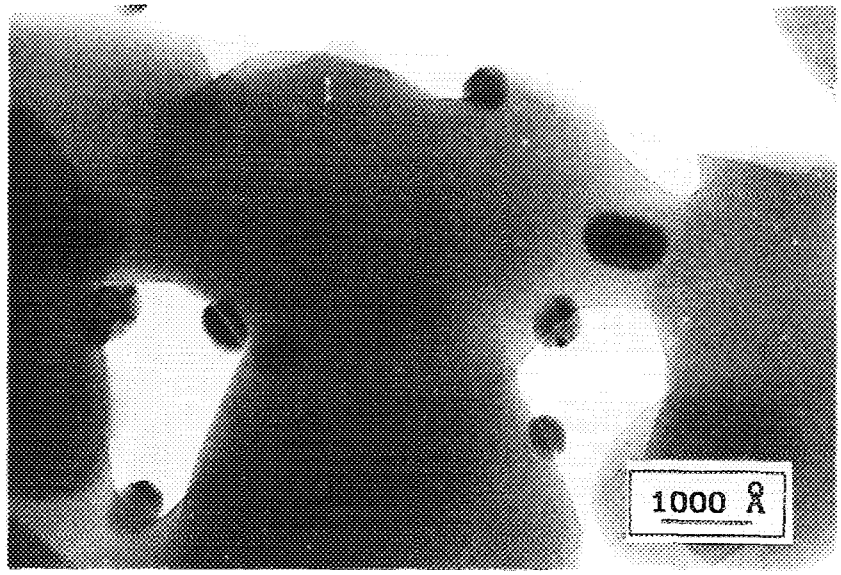

FIG. 2. Typical micrograph of a silver supported catalyst.

arrows in Fig. 4) in the vicinities of which the structure is deformed, in comparison with the perfect crystal lattice observed in each microcrystalline grain.

Thus, we consider the ratio $D_{TEM}/D_{X\text{-}ray}$ as a parameter indicative of the relationship between the regular and imperfect structural regions in the volume of the silver particle. This ratio is a measure of the mean value of microcrystalline domains which compose the Ag particle of mean size, and the expression $n = (D_{TEM}/D_{X\text{-}ray}) - 1$ gives the number of intergrain boundaries.

It should be noted that for small Ag particles from all initial catalysts in question the micrograined structure was not observed. The $D_{TEM}/D_{X\text{-}ray}$ value for these particles is very close to 1 (see Table 2). When D_{TEM} increases, $D_{X\text{-}ray}$ also increases, but to a lesser extent.

Thus, the typical defects in the crystal structure of Ag particles from the initial catalysts investigated are stacking faults and intergrain boundaries; the amount of the latter increases with an increase in silver particle sizes. But an important question arises: how does the real struc-

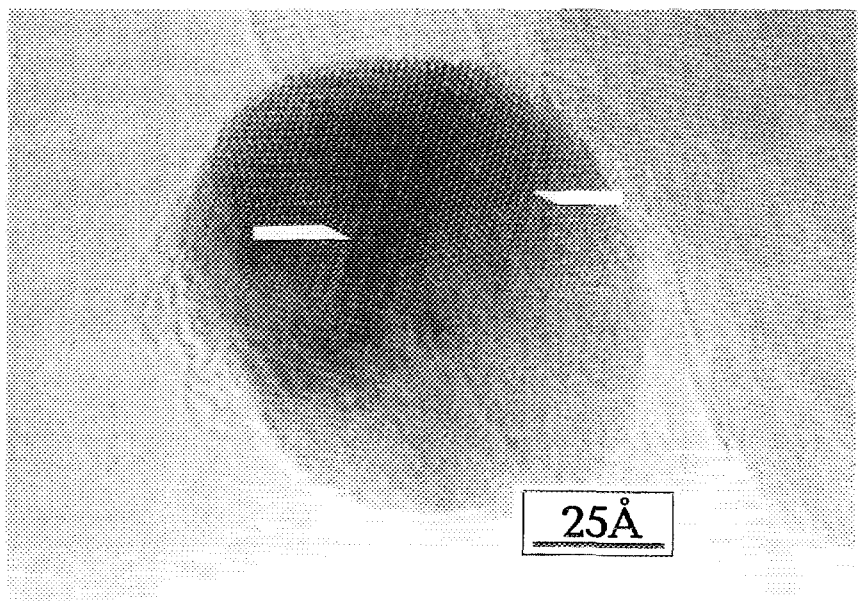

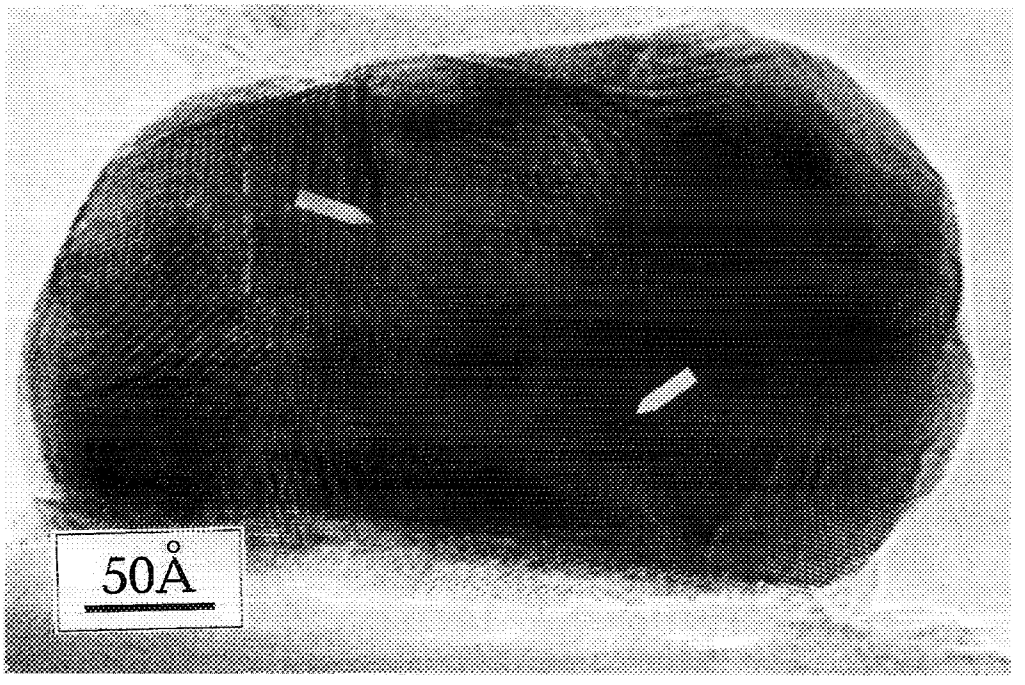

FIG. 4. High resolution electron microscopic image of a silver microcrystal possessing micrograined structure (sample No. 7). Regions with intergrain boundaries are indicated by arrows.

ture of the catalysts change after the catalysts are treated in reaction media? To get an answer to this question, we carried out *in situ* investigations of samples in the thermochamber fitted onto the X-ray diffractometer.

Investigations were performed in air and in the reaction mixture. Diffraction peaks 111, 200, and 220 were recorded at room temperature before the specimen was heated, at 230°C, and at room temperature after the specimen cooled. Data on the broadening of X-ray peaks are listed in Table 3. Results of the experiments in air and in the reaction mixture were identical; therefore data given in Table 3 may be considered common to both cases.

We could not measure the halfwidth of the 111 diffraction peak, because it overlaps with an α-alumina reflection. However, we suggest that the halfwidth of the 111 peak during specimen heating in the X-ray thermochamber is identical with that observed after specimen cooling. This supposition seems to be valid, because there is no significant difference between the halfwidths of the 200 and 220 diffraction peaks detected during heating and after cooling of the catalysts. Silver particles in all the samples in question have a spherical shape, and in this case $D_{X\text{-ray}}$ values in different crystallographic directions are conjugate.

TEM analysis of the real structure of catalysts after *in situ* study was also carried out.

TABLE 3

Data on the Broadening of X-Ray Diffraction Spectra Obtained for *in Situ* Analysis

Sample number	Halfwidth of diffraction peaks, 2θ (°)								
	Initial			Heated, 230°C			Cooled		
	111	200	220	111	200	220	111	200	220
1	0.62	—	0.75	—	0.60	0.70	0.60	—	0.70
5	0.42	0.63	0.70	—	0.53	0.61	0.40	0.53	0.61
7	0.34	0.48	0.44	—	0.40	0.40	0.32	0.40	0.40
8	0.32	0.38	0.38	—	0.35	0.36	0.31	0.35	0.36

Some conclusions which may be drawn from the results of the *in situ* study are as follows:

(i) A decrease in the halfwidths of the 200 and 220 peaks when the specimen is heated indicates improvement of the bulk structure of silver particles. Halfwidths of these reflections are sensitive to the concentration of stacking faults to a greater extent than that of the 111 reflection. We may conclude that stacking faults are annealed under the reaction conditions in all investigated catalysts except Sample 1, where the defects are most stable, probably due to their high concentration.

(ii) Change in the halfwidths of the 200 and 220 reflections is irreversible.

(iii) We did not observe a significant increase in $D_{X\text{-ray}}$ values, because the halfwidths of 111 peaks did not change noticeably. Thus, the micrograined structure already formed at the stage of catalyst preparation is retained throughout the reaction conditions during the experiment.

TEM analysis indicated that after *in situ* treatment of the catalysts, the shape of the silver particles did not change. A noticeable increase in mean particle size was not observed, but the concentration of stacking faults in the structure of the Ag microcrystals sharply decreased, which is consistent with X-ray diffraction measurements.

DISCUSSION

Results of our investigation revealed that a crucial peculiarity of the real structure of Ag particles is associated with the microcrystalline domains and their sizes. Stacking faults, as evident from *in situ* data, are unstable and annealed under the reaction conditions.

Let us return to the main goal of our study, the elucidation of the relationship between the features of the structural arrangement of Ag particles and their sizes. The first fact that attracts attention is the increase of $D_{X\text{-ray}}$ values in that range of true sizes of Ag particles (D_{TEM} = 300–800 Å) for which an increase in catalytic activity is observed. For larger (more than 1000 Å) particles $D_{X\text{-ray}}$ values change slightly, from 600 to 860 Å for Ag particles lying in the range from 1000 to 20,000 Å. This is in accordance with an equally small increase in the catalytic activity.

One could suppose that a number of active centers are associated with $D_{X\text{-ray}}$ values, i.e., the sizes of the regions with a regular structure. However, this seems unlikely because some of the obtained data are in contradiction with the above suggestion. Thus, samples 3 and 4 have a low catalytic activity, though the character of their structure is close to a perfect arrangement. At the same time, sample 6 has the same $D_{X\text{-ray}}$ values as those of sample 4, but the catalytic activity of the sample 6 is high. The difference between these specimens lies in the fact that all the Ag particles in samples 3 and 4 consist of one microcrystalline domain ($D_{TEM}/D_{X\text{-ray}}$ = 0.9), whereas some part of the silver microcrystals in sample 6 is composed of two or more coherent grains ($D_{TEM}/D_{X\text{-ray}}$ = 1.4).

Thus, the increase in size of the regions with a regular crystal structure in Ag particles cannot be the reason for the increase in the catalytic activity. The simultaneous presence of the regular and defect structural regions in silver particles seems to be a likely way for active centers of catalysis to form. Such a situation may be realized when one can synthesize Ag particles consisting of microcrystalline domains separated by intergrain boundaries in the vicinity of which the structure is disturbed.

Figure 5 shows a plot of the epoxidation rate versus $D_{TEM}/D_{X\text{-ray}}$ values. One can see that there is a definite correlation between the rate of the epoxidation reaction and the number of coherent microcrystalline domains and, consequently, intergrain boundaries in the structure of silver particles. When the ratio $D_{TEM}/D_{X\text{-ray}}$ is increased from 0.9 to 1.7, the catalytic activity also increases. According to TEM data and $D_{TEM}/D_{X\text{-ray}}$ values, almost all Ag particles consist of two coherent domains separated by intergrain boundaries in samples 7 and 8.

An increase in Ag particle size (to more than 1000 Å) does not lead to a substantial increase in catalytic activity. In this case silver particles are composed of several coherent domains. Though the number of intergrain boundaries formally increases to a some extent, their density (i.e., the number of intergrain boundaries related to the true particle size) remains constant due to an insignificant increase in $D_{X\text{-ray}}$. Moreover, in large silver particles some intergrain boundaries do not exit onto the particle surface, but localize within the bulk of the Ag microcrystals, forming internal defect regions.

Thus, one can see that the highest catalytic activity is observed for the samples with Ag particles possessing

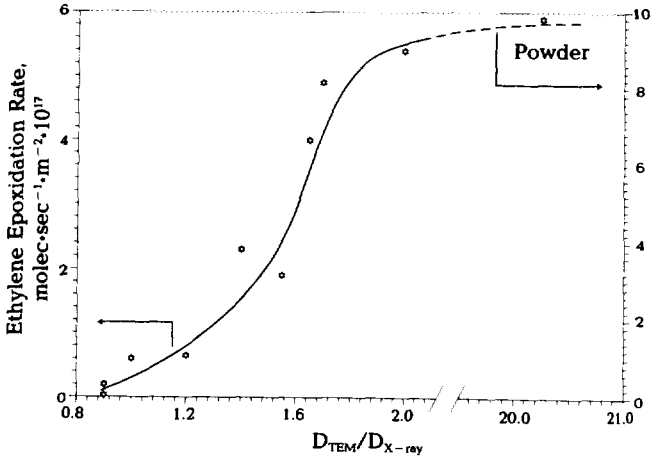

FIG. 5. Plot of the reaction rate of ethylene epoxidation versus $D_{TEM}/D_{X\text{-ray}}$ values.

intergrain boundaries in their structure. The micrograined structure of the Ag particles may be a factor that establishes control over the ratio between the regular and imperfect regions of the surface of silver microcrystals. The latter also seems to be a reason for the observed size effect (8).

A micrograined structure of silver may be obtained at the stage of catalyst preparation as well as directly during catalyst treatment with the reaction mixture, during which the silver particles usually coalesce (18). It is not surprising that in the latter case the formation of intergrain boundaries is possible.

We feel that it is important to emphasize that linear (D_{TEM}) and bulk ($D_{X\text{-ray}}$) sizes of silver particles depend on the parameters of the particle size distribution as well as on particle shape in different ways. It is possible to use the $D_{TEM}/D_{X\text{-ray}}$ ratio as a value characterizing the number of intergrain boundaries in the structure of silver particles only in the case of a narrow particle size distribution, which applies for the samples in question. Nevertheless, even in this case one could not avoid the error introduced by the parameters of size distribution, i.e., type and width of the distribution curve. Therefore, the $D_{TEM}/D_{X\text{-ray}}$ ratio dependence of the epoxidation rate has a semiquantitative character.

We would like to demonstrate the validity of the qualitative correlation between the catalytic properties of Ag particles and parameters of their bulk structure, mainly the microcrystalline domains. At this step in our investigation we are unlikely to be close to a final conclusion about the following problem: are the catalytic active centers formed directly in the vicinity of the intergrain boundaries or is an optimal ratio between the regular and defect regions in the bulk structure of Ag particles needed for the attainment of the active state of the catalysts? To check the validity of the above-mentioned suppositions, additional experiments are required. It would be useful to synthesize catalysts with different sizes of silver particles, but similar $D_{TEM}/D_{X\text{-ray}}$ values. The results of such an investigation will be published in a forthcoming paper.

CONCLUSIONS

The following conclusions can be reached from the results of our investigations of the real structure of silver supported catalysts characterized by different dispersity:

(i) Stacking faults are a main type of defects in the structure of Ag particles in the majority of the samples in question.

(ii) Relatively large silver particles (more than 400 Å) possess a micrograined structure, which is not observed for Ag microcrystals with sizes in the range from 200 to 300 Å.

(iii) The micrograined structure of silver particles is preserved, whereas stacking faults are annealed during *in situ* X-ray study.

(iv) A relationship has been found between the rate of epoxidation reaction and the parameter $D_{TEM}/D_{X\text{-ray}}$. The latter is proportional to the mean value of microcrystalline domains in the structure of silver particle and, consequently, the amount of intergrain boundaries. The observed correlation seems to be associated with a possible influence of the bulk structure of silver particles on their surface arrangement.

REFERENCES

1. Harriott, P., *J. Catal.* **21,** 56 (1971).
2. Wu, J. C., Harriott, P., *J. Catal.* **39,** 395 (1975).
3. Jarjoui, M., Moraveck, B., Gravelle, P. C., Teichner, S. J., *J. Chim. Phys.* **76,** 1061 (1978).
4. Jarjoui, M., Gravelle, P. C., Teichner, S. J., *J. Chim. Phys.* **75,** 1069 (1978).
5. Verykios, X. E., Stein, F. P., Couglin, R. W., *J. Catal.* **66,** 368 (1980).
6. Cheng, S., Clearfield, A., *J. Catal.* **94,** 455 (1985).
7. Seyedmonir, S. R., Plischke, J. K., Vannice, M. A., and Young, H. W., *J. Catal.* **123,** 534 (1990).
8. Goncharova, S. N., Paukshtis, E. A., Bal'zhinimaev, B. S., submitted for publication.
9. Mastikhin, V. M., Goncharova, S. N., Tapilin, V. M., Terskikh, V. V., Bal'zhinimaev, B. S., *J. Mol. Catal.*, to appear.
10. Bukhtiyarov, V. I., Prosvirin, I. P., Kvon, R., Goncharova, S. N., Bal'zhinimaev, B. S., *J. Phys. Chem.*, to appear.
11. Palmer, M. B., Vannice, M. A., *J. Chem. Technol. Biotechnol.* **30,** 205 (1980).
12. Yazykov, N. A., Simonov, A. D., Ermolaev, V. K., and Yudanov, V. F., React. Kinet. *Catal. Lett.* **43,** 565 (1991).
13. Goncharova, S. N., Khasin, A. V., Filimonova, S. S., Bulushev, D. A., *Kinet. Katal.* **32,** 852 (1991). [in Russian]
14. Shmakov, A. N., Mytnichenko, S. V., Tsybulya, S. V., Solovyeva, L. P., Tolochko, B. P., *J. Struct. Chem.* **35,** 85 (1994). [in Russian]
15. Adler, R. P., Otte, H. M., Wagner, G. N., *J. Met. Trans.* **1,** 2375 (1970).
16. JCPDS Data file No. 4-0783.
17. Warren, B. E., Warekois, E. P., *Acta Metall.* **3,** 433 (1955).
18. Ruckenstein, E., and Lee, S. H., *J. Catal.* **109,** 100 (1988).